

**Magic numbers in the neutron-rich oxygen isotopes**B. Alex Brown<sup>1,\*</sup> and W. A. Richter<sup>2,†</sup><sup>1</sup>*Department of Physics and Astronomy, and National Superconducting Cyclotron Laboratory, Michigan State University, East Lansing, Michigan 48824-1321, USA*<sup>2</sup>*Department of Physics, University of the Western Cape, Private Bag X17, Bellville 7535, South Africa*

(Received 31 August 2005; published 21 November 2005)

The predicted and experimental properties of the new doubly magic nuclei  $^{22}\text{O}$  and  $^{24}\text{O}$  are discussed. These together with previous observations lead to a new rule for magic numbers: if there is an oscillator magic number (2, 8, 20, or 40) for one kind of nucleon, then the other kind of nucleon has a magic number for the filling of every possible  $(n, l, j)$  value.

DOI: [10.1103/PhysRevC.72.057301](https://doi.org/10.1103/PhysRevC.72.057301)

PACS number(s): 27.30.+t, 21.60.Cs

In this article we report on the theoretical implications for new magic nuclei that have recently been discovered in the neutron-rich oxygen isotopes ( $Z = 8$ ) out to the neutron drip line at neutron number  $N = 16$ . The single-particle shell structure of nuclei provides the bridge for understanding the rich features of these mesoscopic systems in terms of the interactions between nucleons. On one hand, one would like to derive the shell structure from the basic interactions; on the other hand, one can use the smaller number of single-particle degrees of freedom to derive more complex properties in terms of configuration mixing. An important feature of the shell structures in all mesoscopic systems composed of fermions is the presence of gaps in the single-particle spectra. The magic numbers 2, 8, 20, 28, 50, 82, and 126 associated with the filling of the nucleon orbitals up to the shell gaps in nuclei near stability are well established [1]. For nuclei away from stability the shell gaps can change as in the case of the  $N = 20$  gap for nuclei around  $^{32}\text{Mg}$  resulting in the “island of inversion” [2] for this mass region. Recent experiments have indicated that the spin-orbit interaction decreases with increasing neutron number [3]. Although the  $N$  and  $Z$  dependence of the magic numbers can be qualitatively understood in terms of phenomenological mean-field models, a quantitative connection with the basic interactions between nucleons is still lacking. Recent results from the *ab initio* models of nuclei up to  $A = 12$  suggest that the three-body interactions are important [4].

The oxygen isotopes are the heaviest nuclei for which the neutron drip line has been experimentally well established [5]. The ground states of nuclei inside the drip line have lifetimes that are typical of those for  $\beta$  decay (a few hundred milliseconds in this mass region), and those outside the drip line have lifetimes characteristic of the strong interaction of unbound neutrons with nuclei ( $10^{-21}\text{s}$ ). Thus, in an experiment in which exotic nuclei are produced in the spallation of a heavy nucleus with a target, nuclei inside the drip line can be separated by a mass spectrometer and their properties can be studied in a detector far from the target, whereas nuclei outside the drip line decay immediately in the target. This

technique has been used to show that nuclei up to  $^{24}\text{O}$  are inside the drip line and that  $^{25}\text{O}$  [6,7],  $^{26}\text{O}$  [8,9],  $^{27}\text{O}$  [10] and even  $^{28}\text{O}$  [11] are outside the drip line.

Neutron separation energies for the oxygen isotopes (the least amount of energy it takes to remove either one or two neutrons) are shown in Fig. 1. The experimental values deduced from the measured masses [12] shown in the top panel show the typical odd-even oscillation associated with the pairing interaction between neutrons. Beyond  $N = 16$  the nuclei are outside the drip line and the neutron separation energy becomes negative. A consequence of the small neutron separation energy just inside the drip line is that there are few if any excited states that are bound to  $\gamma$  decay. The experimental values for the neutron separation energy are compared to theoretical calculations in Fig. 1. The theory starts with the observed doubly magic property of  $^{16}\text{O}$ , where there is a shell gap for both protons and neutrons ( $Z = N = 8$ ). The properties of low-lying states of oxygen are obtained from a Hamiltonian for neutrons in the  $0d_{5/2}$ ,  $0d_{3/2}$ , and  $1s_{1/2}$  (*sd*) orbitals with the single-particle energies observed in  $^{17}\text{O}$ . The orbitals are labeled by  $n\ell_j$ , where  $n$  is the number of times the radial wave function crosses zero,  $\ell$  is the orbital angular momentum, and  $j$  is the total (orbital plus spin) angular momentum. The middle panel shows results obtained with a phenomenological one-boson exchange potential (OBEP) [13] two-body interaction, and the bottom panel shows the results obtained with the renormalized  $G$  matrix for the Bonn-A nucleon-nucleon potential [14]. The agreement with experiment is good for OBEP with the neutron drip line at  $N = 16$ . With the Bonn-A  $G$  matrix the drip line is extended to  $N = 20$  in disagreement with experiment.

The energy of the first-excited  $2^+$  state is one of the indicators for magic nuclei. The experimental values for nuclei out to  $^{22}\text{O}$  are shown in the top panel of Fig. 1. The doubly magic nature of  $^{22}\text{O}$  was first indicated by a radioactive beam Coulomb excitation experiment at the National Superconducting Cyclotron Laboratory at Michigan State University [15] where a  $2^+$  state was observed at 3.19 MeV, which is almost twice that in the adjacent  $N = 10$  and 12 nuclei, indicating the presence of a  $N = 14$  shell gap. This is also supported by the  $B(E2)$  value deduced from the inelastic scattering experiments [15]. The absence of any excited states that are bound to  $\gamma$  decay for  $^{24}\text{O}$  observed in

\*Electronic address: brown@nsl.msu.edu

†Electronic address: richter@sun.ac.za

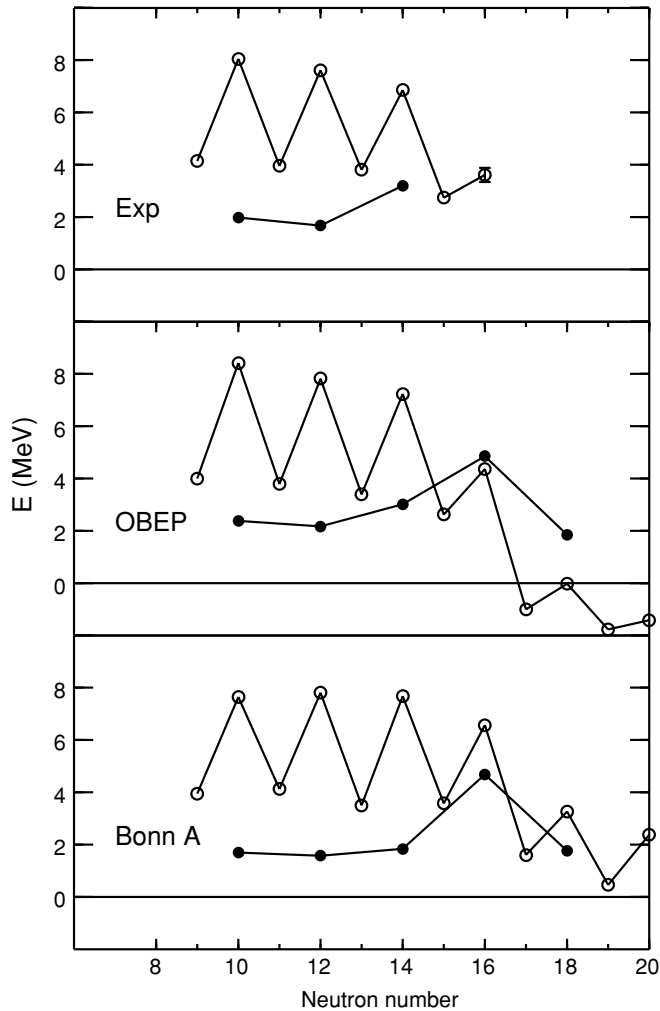


FIG. 1. Excitation energy of  $2^+$  states in even-even nuclei (filled circles) and the neutron separation energies (open circles) for the oxygen isotopes starting at  $N = 9$ . The top panel shows the experimental values, the middle panel are those obtained from the OBEP Hamiltonian and the lower panel are those obtained with the Bonn-A renormalized  $G$  matrix. For the top panel the neutron separation energy beyond  $N = 16$  has not been measured, but they are known to be negative (they are unbound to neutron decay).

experiments at GANIL [16] imply that its first excited state lies above the neutron separation energy of  $3.6 \pm 0.3$  MeV. The OBEP and Bonn-A results for the  $2^+$  energies are also shown in Fig. 1.

The nucleus  $^{24}\text{O}$  ( $N = 16$ ) has very interesting properties. It lies on the neutron drip line but has a relatively large neutron separation energy of 3.6 MeV. There is a sudden drop in the neutron separation energy from 3.6 MeV for  $N = 16$  to a negative value for  $N = 17$ . The lower limit of 3.6 MeV for a bound excited state implies a doubly magic property.

The essential difference between the OBEP and the renormalized  $G$  matrix results can be interpreted in terms of the underlying single-particle degrees of freedom. The single-particle energies as a function of neutron number are shown in Fig. 2. The lowest-energy states filled according to the Pauli principle is  $0d_{5/2}$  between  $N = 9$  and 14,  $1s_{1/2}$

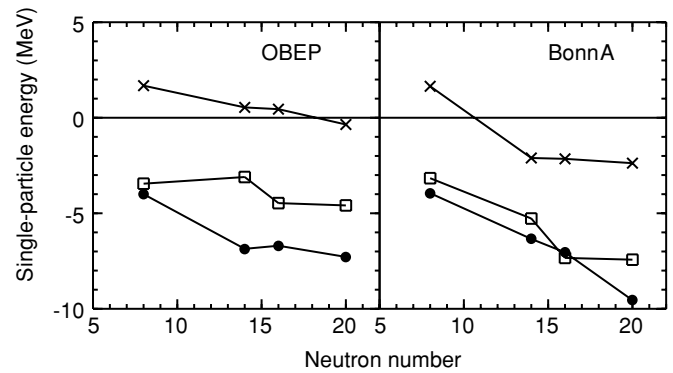


FIG. 2. Single-particle energies for the oxygen isotopes as a function of neutron number. The values obtained for the OBEP and Bonn-A interactions for the  $0d_{5/2}$  orbital (filled circles), the  $1s_{1/2}$  orbital (open squares), and the  $0d_{3/2}$  orbital (crosses) at  $N = 8, 14, 16,$  and 20 are connected by lines.

between  $N = 15$  and 16, and  $0d_{3/2}$  between  $N = 17$  and 20. The increase of the splitting between the  $0d_{5/2}$  and  $1s_{1/2}$  energies between  $N = 9$  and  $N = 14$  found for the OBEP interaction is responsible for creating the shell gap at  $N = 14$  and does not appear for Bonn-A. The loosely bound nature of the  $0d_{3/2}$  orbit for  $N > 16$  found for the OBEP interaction is responsible for making these nuclei unbound to neutron decay.

The incorrect behavior of the  $0d_{5/2} - 1s_{1/2}$  splitting found for the  $G$ -matrix interaction was already indicated in the  $sd$  shell nuclei closer to stability in the early many-particle shell-model calculations for this mass region [17]. This was one of several problems with the renormalized  $G$ -matrix interactions that lead the development of effective two-body matrix elements for the  $sd$  shell that culminated in the set of “universal  $sd$ ” (USD) two-body matrix elements [18]. There are 63 unique combinations of two-body matrix elements for the  $sd$  shell. When the USD values for these are used for configuration mixing, on the order of one thousand low-lying levels in the mass region  $A = 16$ –40 can be reproduced to an rms accuracy of about 200 keV. The OBEP interaction we use here (the SDPOTA interaction in Table XIII of Ref. [13]) was a later successful attempt to fit the  $sd$ -shell energy data in terms of a one-boson exchange potential with fewer (20) parameters. A density dependence was introduced and one of the terms used for the OBEP has an infinite range and is equivalent to a constant (monopole) interaction.

The difference between the OBEP and Bonn-A shell gaps at  $N = 14$  has a dramatic effect on the excited state spectrum of  $^{22}\text{O}$  as shown in comparison with experiment [16] in Fig. 3. The spins of the excited states are not measured experimentally, but the  $\gamma$  decay scheme is consistent with the association between OBEP and experiment indicated in Fig. 3. The Bonn-A spectrum is much too compressed compared to experiment. Excited state spectra for  $^{21}\text{O}$  and  $^{22}\text{O}$  are shown in Ref. [16], where excellent agreement between experiment, and the USD prediction is found. From  $^{18}\text{O}$  to  $^{24}\text{O}$  the results of USD and OBEP are very similar. However, with the USD Hamiltonian  $^{26}\text{O}$  is bound by about 1 MeV, in contradiction to experiment. For the OBEP Hamiltonian  $^{26}\text{O}$  is unbound, in agreement with experiment, but only by about

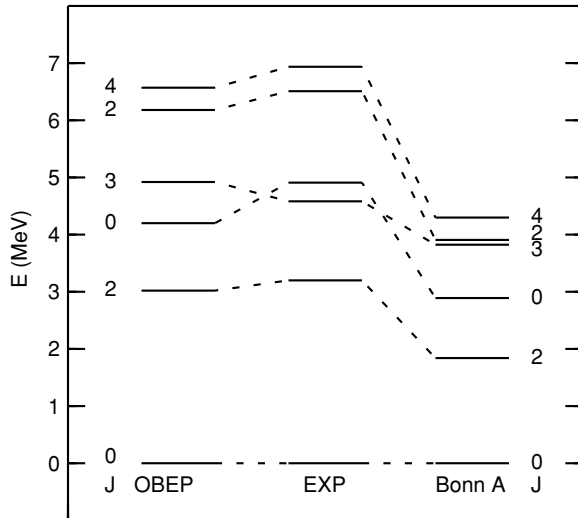


FIG. 3. Energy levels of  $^{22}\text{O}$ . The middle panel shows the experimental energy levels observed in experiment. The left panel shows the results from the OBEP Hamiltonian joined with the experimental levels whose  $\gamma$ -decay properties decay are consistent with theory. The right panel shows the results from the Bonn-A renormalized  $G$ -matrix Hamiltonian.

50 keV. We conclude that shell-model extrapolations to nuclei at and beyond the neutron drip line can be successful if the effective Hamiltonian is well established. The behavior of the single-particle energies is entirely determined by the monopole part of the interaction. The difference between Bonn-A and OBEP (USD) corresponds to a 0.5 MeV increase in the monopole part of the  $0d_{5/2}$ - $1s_{1/2}$  two-body matrix elements. Where does this come from? Zuker has emphasized that these types of effective monopole corrections are also important in the  $p$  and  $pf$  shells and proposes that they may be interpreted in terms of a contribution of the three-body interaction to the valence shell-model interaction [19]. It will be important to find the effect of “realistic” three-body interactions in the shell structure of nuclei as well as in nuclear matter. There does not appear to be any evidence for a decrease in the  $0d_{5/2}$ - $0d_{3/2}$  spin-orbit splitting in contrast to the recent evidence for a decrease found in heavy nuclei [3]. Hartree-Fock models also fail to reproduce the neutron-number dependence of the single-particle energies. This is illustrated in Fig. 4, where the USD single-particle energies (that are similar to the OBEP values in Fig. 2) are compared with typical Woods-Saxon, nonrelativistic Skyrme Hartree-Fock (SKX) [20], and relativistic Hartree-Fock (NL3) [21] results. We have proposed that Hartree-Fock single-particle energies can be combined with shell-model configuration mixing [22]. Although this is necessary for the nuclei far from stability where there is no experimental information on the single-particle energies, it is better to use the effective shell-model Hamiltonians that include the monopole corrections when they can be well determined from experimental data. When the continuum is included in the calculation [23], the states above the neutron separation energy (including the ground states for nuclei beyond the drip line) acquire a decay width because of the one- and two-neutron decay modes. Because the  $0d_{3/2}$

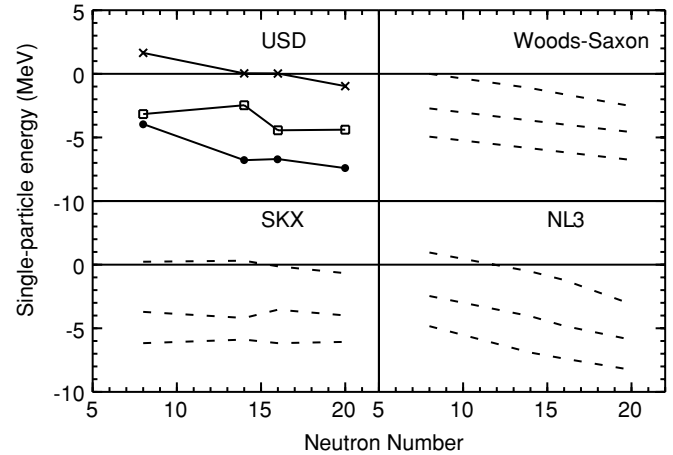


FIG. 4. Single-particle energies as a function of neutron number for the USD effective interaction compared to those obtained with Woods-Saxon, SKX Skyrme Hartree-Fock [20] and NL3 relativistic Hartree-Fock [21] potentials. The order of the orbitals for all panels are  $0d_{5/2}$  (bottom),  $1s_{1/2}$  (middle), and  $0d_{3/2}$  (top).

orbital with a single-particle energy near zero is being filled beyond  $N = 16$ , many of these widths could be narrow—a few hundred kilo-electron volts—because of the low decay energy and the  $\ell = 2$  centrifugal barrier. Thus it will be interesting to carry out experiments that explore the structure of these states beyond the drip line by measuring the resonances associated with the outgoing neutrons in coincidence with final states. Two-thirds of the even-even isotopes are doubly magic ( $^{14,16,22,24}\text{O}$ ). In general doubly magic nuclei are not common. The proliferation of doubly magic nuclei for the oxygen isotopes together with those in other light isotopes that have been known for some time can be generalized in terms of a new rule for magic numbers: *if there is an oscillator magic number ( $N_o = 2, 8, \text{ or } 20$ ) for one kind of nucleon, then the other kind of nucleon has a magic number for the filling of every possible single-particle state*. The sequence for  $(N_o, n\ell_j)$  together with the doubly magic nucleus obtained on filling the last orbit is as follows:  $(2, 0s_{1/2})$   $^4\text{He}$ ;  $(2, 0p_{3/2})$   $^8\text{He}$ ;  $(8, 0p_{3/2})$   $^{14}\text{O}$ ;  $(8, 0p_{1/2})$   $^{16}\text{O}$ ;  $(8, 0d_{5/2})$   $^{22}\text{O}$ ;  $(8, 1s_{1/2})$   $^{24}\text{O}$ ;  $(20, 0d_{5/2})$   $^{34}\text{Si}$ ;  $(20, 1s_{1/2})$   $^{36}\text{S}$ ;  $(20, 0d_{3/2})$   $^{40}\text{Ca}$ ;  $(20, 0f_{7/2})$   $^{48}\text{Ca}$ ;  $(20, 1p_{3/2})$   $^{52}\text{Ca}$ . The next nucleus in this sequence would be  $(20, 1p_{1/2})$   $^{54}\text{Ca}$ .  $^{54}\text{Ca}$  has not yet been observed, but extrapolations based on effective Hamiltonians inferred from nearby nuclei indicate that it may also be doubly magic [24,25]. If the oscillator rule is valid, is it an accident or is there some underlying reason perhaps associated with many-body interactions? Studies of the heavier nuclei at the neutron drip lines that will be possible with the next generation of radioactive beam accelerators will provide critical experimental information for these unique mesoscopic systems. The experimental and theoretical understanding of drip line nuclei is also important for nuclear structure input to astrophysical models of the rapid-neutron capture mechanisms for heavy-element formation [26].

Support for this work was provided from U.S. National Science Foundation grant PHY-0244453 and South African NRF ISL grant GUN No. 2068517.

- [1] B. A. Brown, *Prog. Part. Nucl. Phys.* **47**, 517 (2001).
- [2] E. K. Warburton, J. A. Becker, and B. A. Brown, *Phys. Rev. C* **41**, 1147 (1990).
- [3] J. P. Schiffer *et al.*, *Phys. Rev. Lett.* **92**, 162501 (2004); D. Warner, *Nature* **430**, 517 (2004).
- [4] S. C. Pieper, V. R. Pandharipande, R. B. Wiringa, and J. Carlson, *Phys. Rev. C* **64**, 014001 (2001); S. C. Pieper, K. Varga, and R. B. Wiringa, *Phys. Rev. C* **66**, 044310 (2002).
- [5] M. Thoennessen M., *Rep. Prog. Phys.* **67**, 1187 (2004).
- [6] M. Langevin *et al.*, *Phys. Lett.* **B150**, 71 (1985).
- [7] M. Thoennessen *et al.*, *Phys. Rev. C* **68**, 044318 (2003).
- [8] D. Guillemaud-Mueller *et al.*, *Phys. Rev. C* **41**, 937 (1990).
- [9] M. Fauerbach *et al.*, *Phys. Rev. C* **53**, 647 (1996).
- [10] H. Sakurai *et al.*, *Phys. Lett.* **B448**, 180 (1999).
- [11] O. Tarasov *et al.*, *Phys. Lett.* **B409**, 64 (1997).
- [12] G. Audi, A. H. Wapstra, and C. Thibault, *Nucl. Phys.* **A729**, 337 (2003).
- [13] B. A. Brown, W. A. Richter, R. E. Julies, and B. H. Wildenthal, *Ann. Phys.* **182**, 191 (1988).
- [14] M. Hjorth-Jensen, T. T. S. Kuo, and E. Osnes, *Phys. Rep.* **261**, 125 (1995).
- [15] P. G. Thirolf *et al.*, *Phys. Lett.* **B485**, 16 (2000).
- [16] M. Stanoiu *et al.*, *Phys. Rev. C* **69**, 034312 (2004).
- [17] B. A. Brown and B. H. Wildenthal, *Annu. Rev. Nucl. Part. Sci.* **38**, 29 (1988).
- [18] B. H. Wildenthal, *Prog. Part. Nucl. Phys.* **11**, 5 (1984).
- [19] A. P. Zuker, *Phys. Rev. Lett.* **90**, 042502 (2003).
- [20] B. A. Brown, *Phys. Rev. C* **58**, 220 (1998).
- [21] G. A. Lalazissis, J. König, and P. Ring, *Phys. Rev. C* **55**, 540 (1997).
- [22] B. A. Brown and W. A. Richter, *Phys. Rev. C* **58**, 2099 (1998).
- [23] A. Volya and V. Zelevinsky, *Phys. Rev. Lett.* **94**, 052501 (2005).
- [24] M. Honma, T. Otsuka, B. A. Brown, and T. Mizusaki, *Phys. Rev. C* **65**, 061301(R) (2002).
- [25] S. N. Liddick *et al.*, *Phys. Rev. Lett.* **92**, 072502 (2004).
- [26] J. J. Cowan and F.-K. Thielemann, *Phys. Today* **57**, 47 (2004).